PUBLICATIONS OF THE ASTRONOMICAL SOCIETY OF THE PACIFIC, **120**:644–654, 2008 May

The StarScan Plate Measuring Machine: Overview and Calibrations

N. ZACHARIAS, L. WINTER,[1] E. R. HOLDENRIED,[2] J.-P. DE CUYPER,[3] T. J. RAFFERTY,[2] AND G. L. WYCOFF

U.S. Naval Observatory, Washington, DC 20392; nz@usno.navy.mil

Received 2008 March 17; accepted 2008 April 22; published 2008 May 28

ABSTRACT. The StarScan machine at the U.S. Naval Observatory (USNO) completed measuring photographic astrograph plates to allow determination of proper motions for the USNO CCD Astrograph Catalog (UCAC) program. All applicable 1940 AGK2 plates, about 2200 Hamburg Zone Astrograph plates, 900 Black Birch (USNO Twin Astrograph) plates, and 300 Lick Astrograph plates have been measured. StarScan comprises a CCD camera, a telecentric lens, an air-bearing granite table, stepper motor screws, and Heidenhain scales to operate in a step-stare mode. The repeatability of StarScan measures is about 0.2 μm. The CCD mapping as well as the global table coordinate system has been calibrated using a special dot calibration plate and the overall accuracy of StarScan x, y data is derived to be 0.5 μm. Application to real photographic plate data shows that position information of at least 0.65 μm accuracy can be extracted from coarse-grain 103a-type emulsion astrometric plates. Transformations between "direct" and "reverse" measures of fine-grain emulsion plate measures are obtained on the 0.3 μm level per well-exposed stellar image and coordinate, a level that is at the limit of the StarScan machine.

1. INTRODUCTION

This paper introduces the current StarScan hardware and gives details about its operation, calibration, and scientific program. This effort is part of the IAU Task Force on Preservation and Digitization of Photographic Plates (PDPP)[4] to measure astronomical plates worldwide. Reductions of these astrograph data is in progress, and astrometric results will be presented in an upcoming paper.

The StarScan machine in its original setup was acquired by the U.S. Naval Observatory (USNO), Washington in the 1970s. A projection system (Douglass et al. 1990) was used to determine centroids of stellar images in a semi-automatic mode using a list of target stars to be measured. The Twin Astrograph Catalog (TAC), based on over 4000 plates, resulted from these measures (Douglass et al. 1990; Zacharias & Zacharias 1999). In the early 1990s StarScan operations stopped, and, due only to its extremely large and heavy granite table, the machine was not thrown out, instead being sealed off in a small room in its original building with a new access door to the outside.

Starting in 1998 (Winter & Holdenried 2001) StarScan was completely refurbished, switching to the current operation mode with an imaging CCD camera and step-stare scanning of entire plates. The hardware change was performed by L. Winter (contractor), T. Rafferty (USNO, now retired) and the USNO instrument shop. The new operations software was developed by E. Holdenried (USNO, now retired), and the raw data reduction pipeline was adopted from a similar program at the Hamburg Observatory (L. Winter).

In § 2 of this paper the current science program is described, aiming at early epoch star positions to derive proper motions. Section 3 presents details on the hardware including the 2006 upgrade and § 4 describes the calibration process from setup of dedicated measures to interpretation of results. Section 5 reveals external errors derived from measures of real astrometric plates, and § 6 summarizes the astrometric performance of StarScan.

2. SCIENCE PROGRAM

The current StarScan operation is part of the USNO CCD Astrograph Catalog (UCAC) program (Zacharias et al. 2000, 2004). All-sky, astrometric observations were completed in 2004, and reductions for the final release are in progress. StarScan will provide early epoch positions on the Hipparcos system (ESA 1997) from these new, yet unpublished measures. The UCAC program aims at a global densification of the optical reference frame to magnitude R = 16 including proper motions for galactic dynamics studies. A variety of early epoch data are used for UCAC with the StarScan measures allowing an improvement over Tycho-2 (Høg et al. 2000) and extending to fainter magnitudes at a high accuracy level for a large fraction of the sky.

Table 1 lists the plates in the just-completed StarScan measure program. Most plates were taken with dedicated, astrometric astrographs of about 2 m focal length. AGK2 is the *Astronomische Gesellschaft Katalog* data taken at Hamburg

[1] contractor (sole proprietary), Hamburg, formerly University of Hamburg.
[2] USNO, retired.
[3] Royal Observatory of Belgium, Ukkel, Belgium.
[4] The Web site of the IAU Task Force for the Preservation and Digitization of Photographic Plates can be found at http://www.lizardhollow.net/PDPP.htm.

Report Documentation Page

Form Approved
OMB No. 0704-0188

1. REPORT DATE	2. REPORT TYPE	3. DATES COVERED
MAY 2008		**00-00-2008 to 00-00-2008**

4. TITLE AND SUBTITLE	5a. CONTRACT NUMBER
The StarScan Plate Measuring Machine: Overview and Calibrations	5b. GRANT NUMBER
	5c. PROGRAM ELEMENT NUMBER
6. AUTHOR(S)	5d. PROJECT NUMBER
	5e. TASK NUMBER
	5f. WORK UNIT NUMBER
7. PERFORMING ORGANIZATION NAME(S) AND ADDRESS(ES) **U.S. Naval Observatory,Washington,DC,20392**	8. PERFORMING ORGANIZATION REPORT NUMBER
9. SPONSORING/MONITORING AGENCY NAME(S) AND ADDRESS(ES)	10. SPONSOR/MONITOR'S ACRONYM(S)
	11. SPONSOR/MONITOR'S REPORT NUMBER(S)

12. DISTRIBUTION/AVAILABILITY STATEMENT
Approved for public release; distribution unlimited

13. SUPPLEMENTARY NOTES

14. ABSTRACT

15. SUBJECT TERMS

16. SECURITY CLASSIFICATION OF:			17. LIMITATION OF ABSTRACT	18. NUMBER OF PAGES	19a. NAME OF RESPONSIBLE PERSON
a. REPORT **unclassified**	b. ABSTRACT **unclassified**	c. THIS PAGE **unclassified**	**Same as Report (SAR)**	**11**	

TABLE 1

ASTROMETRIC PLATES IN THE JUST-COMPLETED STARSCAN MEASURE PROGRAM. THE AGK2 COVERS EACH AREA OF THE NORTHERN SKY TWICE (TWOFOLD OVERLAP OF PLATES). THE BY (SOUTH) AND ZA (NORTH) PROGRAMS TOGETHER COVER ABOUT 35% OF THE ENTIRE SKY AREA.

Project, telescope name	AGK2	BY	ZA	Lick
Focal length (meter)	2.0	2.0	2.0	3.75
Plate size (mm)	220 sq.	200×250	240 sq.	240 sq.
Measurable field size (degree)	5×5	5×6	6×6	3×3
Limiting magnitude	B = 12	V = 14	V = 14	V = 15
Number of plates	1940	900	2200	300
Range of epochs	1929–31	1985–90	1977–93	1980–2000
Emulsion type	fine grain	103aG	103aG	various
Declination range (degree)	$-2.5 + 90$	$-90 + 10$	$-5 + 90$	$-20 + 90$
Sky coverage completeness	twofold	35%	35%	5%

and Bonn observatories between 1929 and 1933, covering completely the −2.5° to +90° declination range with a blue limiting magnitude of about 12. In a twofold overlap pattern of plates, each area of the sky in that declination range is observed on two different plates. Only a small fraction of the stars visible on the plates could be measured and reduced in a several-decades-long, manual program to produce the published AGK2 catalog (Schorr & Kohlschütter 1951). The data were then combined with the 1960s re-observations to form the AGK3, which includes proper motions based on ≈30-yr epoch difference between AGK2 and AGK3 plates. Combining the new measures of the 1930 epoch AGK2 data with the UCAC survey at epoch ≈2001 will result in proper motions accurate to about 1 mas yr^{-1}, thus significantly improving upon the Tycho-2 result.

Between 2002 and 2003 all 1940 applicable original AGK2 plates were completely digitized on StarScan. This re-measure effort was carefully planned and prepared by the late Christian de Vegt (1978), Hamburg Observatory. About 40% of these new measures entered the UCAC2 release from preliminary reductions available at the cutoff date. The complete AGK2 data will enter the UCAC3 (in preparation).

The BY, ZA, and Lick columns in Table 1 give details of the Black Birch (USNO Twin Astrograph, New Zealand) Yellow Lens, the Hamburg Zone Astrograph (ZA), and the Lick Astrograph plates, respectively. Most of these BY and ZA plates were taken around radio sources (quasars and radio stars) used in the International Celestial Reference Frame (ICRF), and together they cover about 35% of the sky (both hemispheres). The limiting magnitude is about V = 14. When combined with the more recent CCD observations, proper motions on the 3–5 mas yr^{-1} level can be derived for millions of stars beyond the Tycho-2 limiting magnitude. The Lick astrograph has a more favorable image scale than BY and ZA, and also uses mostly fine-grain emulsions. However, only a limited number of fields were observed during this decade-long test program at an epoch around 1990.

3. STARSCAN DETAILS

3.1. Hardware

Figure 1 shows the StarScan machine as of 2006 July. The granite base measures 2.4 by 1.5 by 0.3 m, and plates up to 2 60 mm × 260 mm can be measured. An x, y-table moves on the base via pressure air bearings while a CCD camera is mounted on a granite crossbeam that is fixed to the base.

A photographic plate is put inside a plate holder on a rotation disk that is mounted on the x, y-table. With emulsion up, the plate is clamped upward against a fixed mechanical reference plane. Thus the location of the plate emulsion is always at the same distance from the lens and no change in focus is required during operations even if different types of plates are being measured. For very thin plates a supporting clear glass plate can be inserted underneath the plate to be measured. The x, y-table is moved by precision screws and stepper motors while the coordinates are read from Zerodur Heidenhain scales to better than 0.1 μm precision.

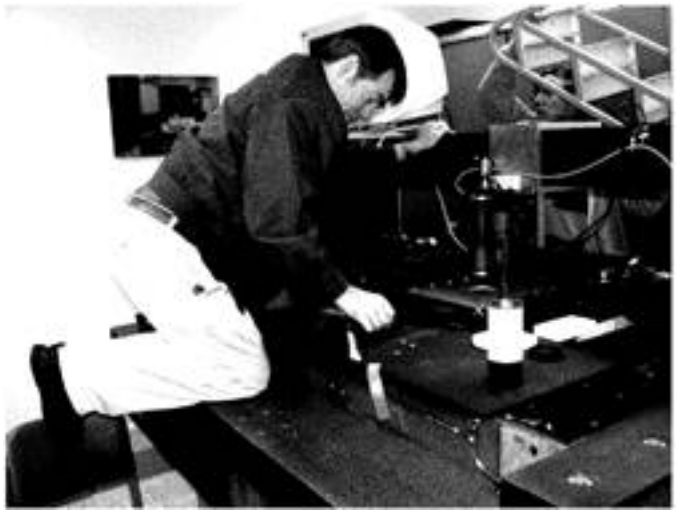

FIG. 1.—StarScan plate measuring machine at USNO, Washington DC, with Lars Winter on top of things and Gary Wieder in the background.

The plate is illuminated from below with a diffuse light projection system and a two-sided telecentric objective (Schneider Xenopla, imaging scale 1:1) maps a section of the plate being measured onto a CCD. From the year 2000 until spring 2006 a Pulnix CCD camera with 1280 by 1030 pixels of 6.7 μm size was used. Thereafter a 2 k by 2 k QImaging camera with 7.4 μm square pixels (Kodak chip) has been used. Figure 2 shows a close-up view of the area with the plate and the new CCD camera attached to the lens.

The new camera was selected to be compatible with the existing system in order to minimize changes. However, the upgrade to the new camera did not go smoothly due to various interface issues and in the end a change of the operating system and a complete rewrite of large portions of the code was required as well as a new mechanical adapter.

3.2. Measure Process

Most functions, including disk rotation and its clamping mechanism are under computer control. At the beginning of each plate measure the illumination is manually set to just below saturation on the plate background by adjusting the power supply unit to the lamp. Then the plate is measured automatically in step-stare mode. The x, y-table moves to the next grid coordinates, the actual table coordinates are obtained by reading out the calibrated Heidenhain scales, a digital image is taken, and another read out of the actual table coordinates is performed. If the table coordinates from the two readings differ by more than 0.1 μm the procedure is repeated. Meanwhile the image is processed: bias, flat field, and dark current corrections, object detection and image profile fits. The entire cycle took about 2.5 s with the old camera and takes about 4.0 s with the new camera, which covers about 3 times more area, resulting in an overall throughput gain of a factor of 2.

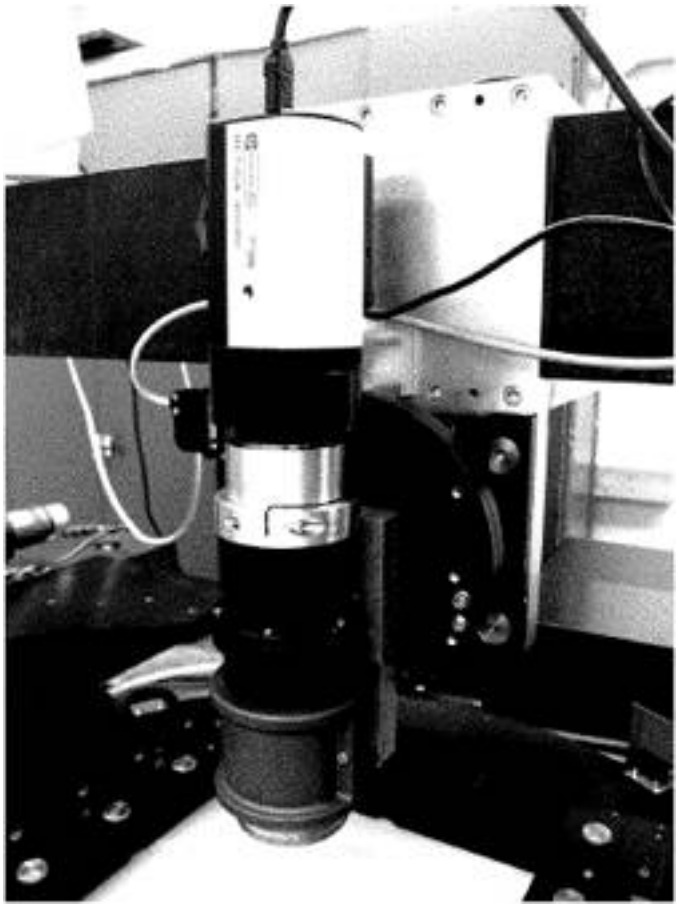

FIG. 2.—Close-up view of the StarScan plate measure area with the 2 k by 2 k QImaging camera and Schneider telecentric lens.

A photographic plate is, thus, digitized to 10 bit with a resolution of now 7.4 μm per pixel. Adjacent pictures have overlap. The usable field-of-view of the old camera was 8.71 by 6.86 mm, while grid steps of about 7.5 and 5.9 mm for x and y, respectively, were used. The new camera has a usable field of about 13×13 mm, with slightly degraded image quality (field curvature) visible in the corners. A grid step size of about 11 mm is adopted between adjacent images.

After the plate measure is complete, the disk is unclamped, rotated by 180°, clamped, and the "reverse" measure started. With the new setup a measure of a single plate in two orientations takes about 45 minutes. All pixel data (about 3.6 GB compressed per plate) are transferred overnight and saved to DVD the following day. The stellar image profile fit results are collected on hard disk for further processing.

3.3. Notes on Reductions

The bias, flat field, and dark current corrected pixel data of the CCD camera are used in two-dimensional fits to obtain centroid coordinates of stellar images. A double exponential model function is used for this purpose (Winter 1999),

$$I(x,y) = B + A(1 - e^{-ln2e^{-[8/(ln2)]S(r-r_0)}}),$$

$$r = \sqrt{(x-x_0)^2 + (y-y_0)^2},$$

with the six independent parameters $B =$ background intensity level, $A =$ amplitude, $x_0, y_0 =$ image centroid coordinates, $r_0 =$ radius of profile, and $S =$ shape parameter. This function models the shape of the observed profiles sufficiently well for all levels of brightness of the stars, while, for example, a simple Gaussian function does not match the saturated bright star profiles with "flat tops" very well. Due to the fine sampling (at least 4 pixels across the diameter of the smallest stellar images) a sufficiently large number of pixels contain signal to determine these six profile parameters per stellar image. The internal fit precision for all well-exposed stars is typically in the order of 0.1 μm or even below for relatively bright, circular symmetric stellar profiles. For quality control, the internal image profile fit errors are plotted versus

the instrumental magnitude for all stellar images of a single plate measure and orientation.

In order to arrive at highly accurate, global x, y coordinates of stellar images from these plate measures several assumptions need to be verified and calibration parameters need to be obtained. Only the center of the CCD chip (or some other, fixed, adopted reference point) is initially associated with the x, y-table coordinate readings from the scales. The positions of arbitrary stellar images measured on the CCD chip field-of-view in pixel coordinates need to be referred to the global, x, y-table coordinates of the machine, i.e., the mapping model and parameters need to be obtained for this transformation. An important parameter here is the third order optical distortion of the telecentric lens. Using the dot calibration plate (see below) StarScan has been set up to give a mapping scale of 1.0 to within $<1\%$ and the CCD pixel coordinates are aligned to the global x, y-table coordinates to within 10^{-4} radian. In addition, geometric distortions of the observed, global, x, y-table coordinates with respect to ideal rectangular coordinates need to be investigated. For both steps, calibrations of the StarScan machine are being made (see below).

Finally, the "direct" and the "reverse" measures of the same plate are compared to check for possible systematic errors, e.g., as a function of magnitude or x, y coordinates introduced by the measuring process, and to verify that the applied mapping procedures were adequate. The direct-minus-reverse residuals also identified several unexplained glitches of some plate measures, which could have been caused by thermal drifts or electronic problems. The set of the reverse measures X, Y (after rotation by 180°) is fit to the direct measures (x, y) with the following transformation model:

$$X = ax + by + c + ex + fy + px^2 + qxy,$$

$$Y = -bx + ay + d + ey - fx + qy^2 + pxy,$$

where a, b, c, and d are the parameters for the orthogonal model, e and f the nonorthogonal, linear parameters, and p and q account for a possible tilt between the two sets of measures. At the precision level investigated here, the rotation axis of the disk is not perfectly perpendicular to the plane of the plate and the p, q terms are required. These tilt terms are reproducible to some extent; however, sometimes a grain of dust would be trapped between the plate and reference plane of the machine, resulting in significantly different tilt terms. It is important to realize that even after applying the above transformation (and averaging of the x, y-coordinates from the direct and the rotated reverse measures) the data set is affected by an unknown tilt, the tilt of the direct measure photographic plate surface with respect to the plane of the x, y-table motion. Thus, for the astrometric reductions to follow (from x, y to α, δ) the minimal plate model has to include tilt terms as well, even if the tangential point would be known precisely and in the absence of a tilt between the optical axis of the telescope and the photographic plate.

4. CALIBRATION

4.1. Dot Calibration Plate

The Royal Observatory of Belgium bought a dot calibration plate (DCP), which was made to specifications for the purpose of calibrating photographic plate measuring machines. This 25 1 mm $\times$ 251 mm $\times$ 4.6 mm glass plate is highly transparent except for circular, opaque, metal dots of ≈ 50 to 300 μm diameter, which are put on the plate in a regular grid covering the inner 240 mm $\times$ 240 mm. Medium-size dots (100 μm) occupy a regular grid of 1.0 mm spacing with small dots (50 μm) put in between every 0.5 mm along both coordinates. In hierarchical order the dots are slightly larger for 5, 10, 50, and 100 mm major grid lines and located at the line intersections of such. The orientation of the grating is uniquely marked by a few out-of-symmetry dots and a missing small dot every centimeter.

The dot calibration plate was manufactured by silicon wafer technology machines and the location of the dots are believed to be accurate to within ≈ 0.1–0.2 μm for both the small-scale regularity and the global, absolute coordinates over the entire area of the plate.

The dots resemble very high-contrast, stellar images and are processed with the standard reduction pipeline at StarScan. The internal position fit errors of these dots are typically 0.1 μm for the medium dots on the 1 mm grid, slightly larger for the small 0.5 mm grid dots, and even smaller for the major grid dots.

4.2. CCD Camera Mapping

Initial StarScan mapping parameters for the CCD pixel coordinates to global x, y-table coordinates transformation are determined from repeated measures of the dot calibration plate, centered on main grid lines and dithered by small offsets in x and y. This in particular allows the determination of the third order optical distortion term D of the lens, which is then used in the preliminary pipeline, together with orientation and scale information, to identify the same star as seen in two or more adjacent, overlapping CCD images. Figure 3 shows the residuals of the 2 k camera optical distortion pattern after removal of that third order term. The working area used for plate measuring is about 11×11 mm. The scale of the residual vectors is 1000, thus the largest residual is about 1.0 μm, with most of the residuals in the 0.1–0.2 μm range. The point-spread function (PSF) of images in the CCD working area is uniform, and there is no variation of the PSF over the area of the plate because there is no variation of best focus over the plate area due to the hardware setup described above.

It is assumed that the mapping parameters stay constant for each individual plate measured in a single orientation; thus, all overlap images of such a data set are used simultaneously to determine the following seven mapping parameters a,b, e, f, p, q, and D from

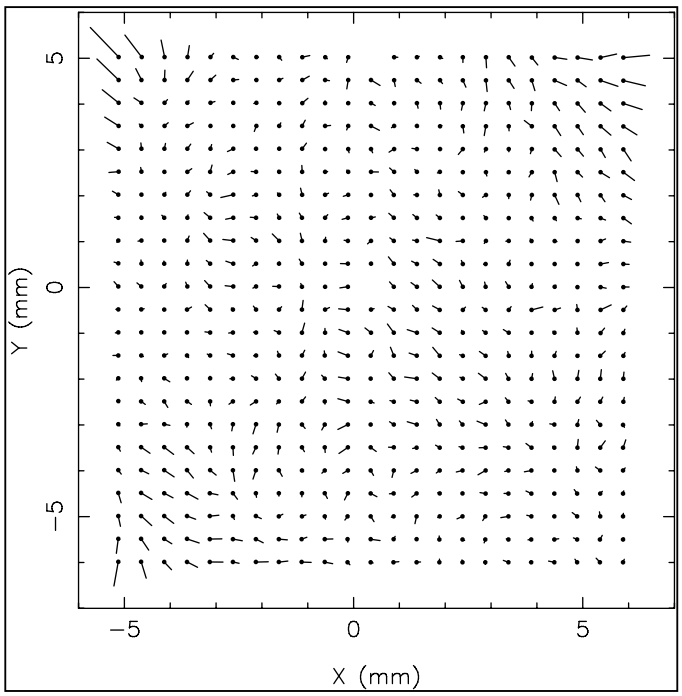

FIG. 3.—Optical distortion pattern of the 2 k camera field of view after removal of the third-order term. The residual vectors are scaled by a factor of 1000; thus, the largest vector is about 1.0 μm long. Results are shown in the $\sim 11 \times 11$ mm area of the detector that is used for plate measuring.

$$\Delta X = ax + by + ex + fy + px^2 + qxy + Dx(x^2 + y^2),$$

$$\Delta Y = -bx + ay + ey - fx + qy^2 + pxy + Dy(x^2 + y^2),$$

where ΔX and ΔY are the coordinates of a star in the global, x, y-table system (in millimeters) with respect to the current position as read by the scales, and x and y are the stellar image coordinates on the CCD (in pixels) with respect to the center of the CCD. The difference between two such equations per coordinate is observed for each pair of overlapping images on two CCD frames of the same star.

There are no constant terms because the zero point of this transformation is arbitrary, thus there are only four linear terms a, b, e, and f. The p and q terms represent the tilt between the plane of the CCD chip inside the camera and the photographic plate. The higher-order terms for distortion and tilt are almost constant for a large number of plates of the same type, and a mean value can be determined and used as fixed parameter in the CCD mapping procedure, while solving then for the linear parameters for each individual plate and orientation measure set with significantly lower errors. Results will be presented in an upcoming paper of this series.

4.3. DCP Measures

The DCP was measured in four orientations (000°, 090°, 180°, and 270°) consecutively with a x, y-table step size of 5 mm, major dot grid lines well centered, and grid lines precisely aligned to the table motion. The entire set of measures was repeated about 2 weeks later, with many regular survey plates measured in between. For the present purpose only the *central dot* of each CCD image has been evaluated, and it fell on the same spot on the CCD chip within about ± 10 pixels. Thus, any errors introduced by the CCD mapping model are negligible, and we measure here the accuracy of the x, y-table coordinates of StarScan. In the following we refer to these sets of measures as *m1c* and *m2c*, each consisting of four single orientation measures of 2025 dots each (on a 220 mm $\times$ 220 mm area with 5 mm step size).

4.4. Repeatability

Without any assumptions on the errors of the DCP, a comparison between two measures of the same dots in the same measure orientation reveals the absolute repeatability of StarScan measures. Using a linear transformation model between the two sets of measures of the 2025 dots gives the results in lines 1 through 4 in Table 2 for the rms observed differences per coordinate. The mean of the four orientations is presented on line 5 and example 2—dim vector plots of the measured position differences are shown in Figure 4. All vectors are small (≈ 0.3 μm) but not randomly oriented. For parts of some lines along x they are highly correlated, mainly affecting the Δx coordinate.

Examples are seen in Figure 4, for the 90° orientation case (*left panel*) for $y = -110$, -100, -30, +40, and +60 mm, and for the 180° case (*right panel*) for $y = -70$, +30, and +50 mm. These glitches are currently not well understood, and seem to appear randomly for a typically length of 50–150 mm along the x axis. Some of these errors will cancel out when combining the direct and reverse measure of a plate. These "glitches" were not further investigated and currently represent the physical limit of the StarScan measure accuracy.

To arrive at the repeatability error ($\sigma_{\rm rep}$) of a single StarScan measure over the entire plate area and per coordinate we divide the rms differences (Table 2, result line 5, showing the scatter between two measures) by $\sqrt{(2)}$ and thus obtain 0.23 and 0.15 μm for the x and y coordinate, respectively. This error is not dominated by the fit precision of the dots, as explained above; instead it shows the limit of accuracy of the x, y-table coordinate measures.

4.5. Corrections to *x*, *y* -Table Coordinates

Next we investigate systematic errors of the x, y-table coordinates, i.e., the global, geometric distortions. For each data set (two measures, each with four orientations) a least-squares fit is performed of the measured coordinates to the nominal, ideal grid coordinates, using the above-mentioned eight-parameter model, which includes linear and tilt terms. Results are presented in Table 2, lines 6 to 13, and for some cases plots are

TABLE 2

RESULTS OF TRANSFORMATIONS BETWEEN TWO SETS OF DATA, DCP IS CALIBRATION PLATE, M1C AND M2C ARE THE SETS 1 AND 2 OF MEASURES OF CENTRAL DOTS, AND 000 TO 270 INDICATE THE ORIENTATION OF A MEASURE. SEE TEXT FOR MORE DETAILS.

Result number	Data set 1	Data set 2	Model	rms x (μm)	rms y (μm)
1	DCP m1c 000	DCP m2c 000	linear	0.31	0.20
2	DCP m1c 090	DCP m2c 090	linear	0.34	0.24
3	DCP m1c 180	DCP m2c 180	linear	0.30	0.15
4	DCP m1c 270	DCP m2c 270	linear	0.33	0.23
5	mean of 1–4			0.32	0.21
6	DCP m1c 000	ideal grid	lin.+ tilt	0.41	0.44
7	DCP m1c 090	ideal grid	lin.+ tilt	0.47	0.53
8	DCP m1c 180	ideal grid	lin.+ tilt	0.36	0.56
9	DCP m1c 270	ideal grid	lin.+ tilt	0.40	0.42
10	DCP m2c 000	ideal grid	lin.+ tilt	0.40	0.40
11	DCP m2c 090	ideal grid	lin.+ tilt	0.44	0.57
12	DCP m2c 180	ideal grid	lin.+ tilt	0.37	0.53
13	DCP m2c 270	ideal grid	lin.+ tilt	0.48	0.40
14	mean, smoothed 2-dim x, y-table corrections			0.27	0.39
15	result 6	mean corrections	none	0.32	0.33
16	result 7	mean corrections	none	0.35	0.23
17	result 8	mean corrections	none	0.28	0.32
18	result 9	mean corrections	none	0.31	0.20
19	result 10	mean corrections	none	0.28	0.32
20	result 11	mean corrections	none	0.30	0.26
21	result 12	mean corrections	none	0.28	0.27
22	result 13	mean corrections	none	0.37	0.27
23	ZA 1929 000	ZA 1930 000	lin.+ tilt	0.89	0.85
24	ZA 1929 180	ZA 1930 180	lin.+ tilt	0.84	0.89
25	ZA 1931 000	ZA 1932 000	lin.+ tilt	0.92	0.92
26	ZA 1931 180	ZA 1932 180	lin.+ tilt	0.92	0.92
27	Lick 724 m1 000	Lick 724 m1 180	lin.+ tilt	0.41	0.68
28	Lick 724 m6 000	Lick 724 m6 180	lin.+ tilt	0.40	0.35
29	Lick 724 m9 000	Lick 724 m9 180	lin.+ tilt	0.42	0.49
30	Lick 724 ma 000	Lick 724 ma 180	lin.+ tilt	0.45	0.45

shown in Figure 5. As can be seen, the difference vectors are highly correlated among the different plots, indicating that the dominating error source is systematics in the StarScan x, y-table geometry, due to imperfections of the axes as the plate is moved along in the measuring process. If the DCP had large errors compared to StarScan, the rotated measures (90° and 180°) would show the same pattern as the direct measure (orientation 0°) but rotated by that angle. However, we see here the systematic error pattern correlated directly to the StarScan x, y coordinates, regardless of the orientation of the calibration plate.

A mean two-dimensional vector difference map was constructed by averaging all eight measures (two sets times four orientations each) and then applying a near neighbor smoothing. Results are given on line 14 in Table 2, and the corresponding vector plot is shown in Figure 6. Subtracting this mean pattern from the individual measure sets (Table 2, lines 6 to 13) results in lines 15 to 22 with rms values almost as low as the StarScan repeatability, showing the successful removal of most of the x, y-table systematic errors.

5. APPLICATION TO REAL DATA

5.1. Different Plates of the Same Field

In order to determine the physical limit of astrograph plates for astrometry, a set of four different plates taken of the same field (2234+282) in the sky is investigated. The four plates were taken in 1988 with the Hamburg Zone Astrograph (ZA; de Vegt 1976) in the same night within 40 minutes off the meridian through an OG515 filter on 103aG emulsion. Plate numbers 1929 and 1930 were taken with the telescope on the west side of the pier, numbers 1931 and 1932 on east. Here we assume that the StarScan measure errors are small and we will try to determine total external errors from the combination of plate geometry (emulsion shifts) over the entire field of view and the background noise from the emulsion grains, using real stellar images.

A transformation of the direct measure of ZA1930 onto the direct measure of ZA1929 was performed using the above-mentioned eight-parameter model and using about 19,000 stellar images in an unweighted, least-squares fit. A five-parameter mapping model including linear and tilt terms was used for

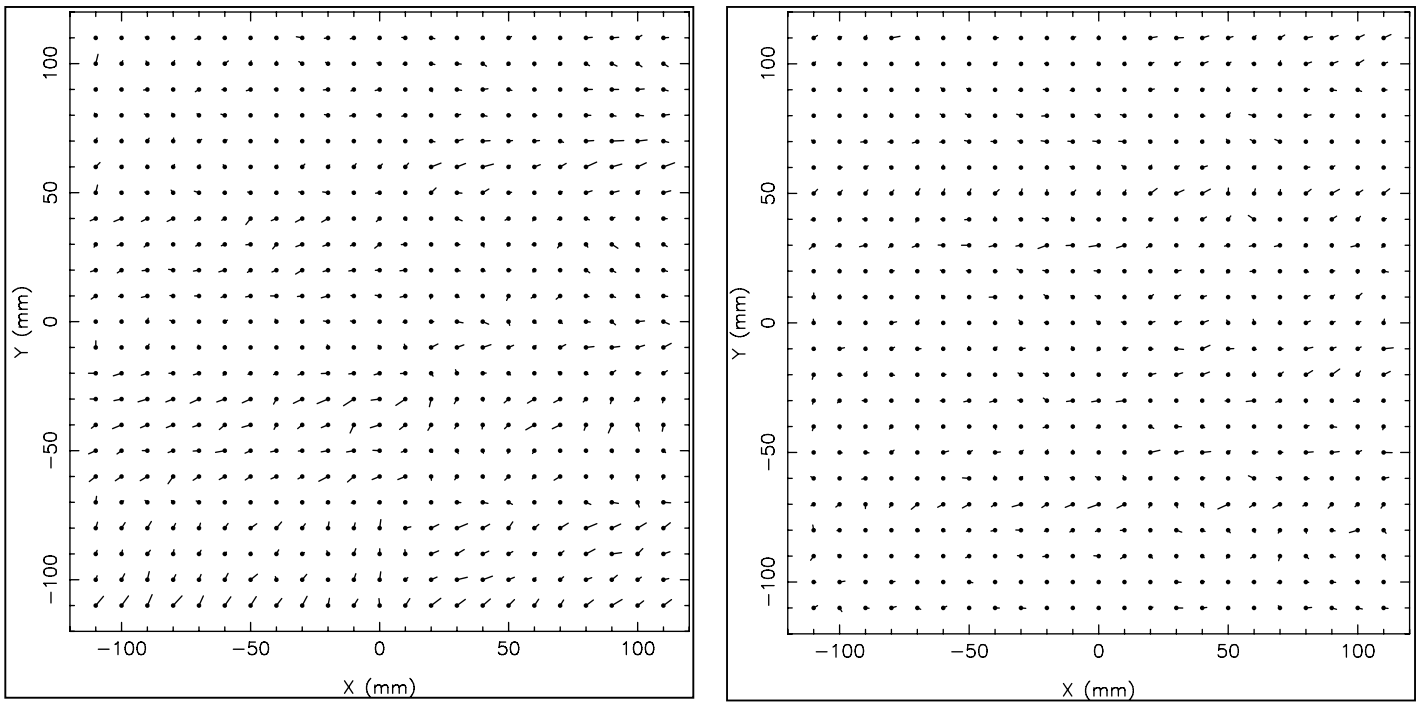

FIG. 4.—Repeatability: vector plot of position differences between two measures of the same dot calibration plate in the same orientation, performed on different days. The examples show the worst (*left panel*) and best (*right panel*) case (90° and 180° orientation, respectively). The scale is 5000; thus, the largest vectors are about 1.0 μm long, and the rms vector length is 0.42 and 0.33 μm, respectively.

the CCD camera mapping, after applying a mean optical distortion term to the raw data. No x, y-table corrections of StarScan were applied because they would cancel anyway in this direct to direct transformation (assuming stability of the machine over the few hours in which the set of plates were measured). Table 2, lines 23 to 26, show the mean rms differences for "well-exposed" stars (about tenth magnitude) between the two plates. Thus, the external error of a single, well-exposed stellar image on a single plate is about 0.65 μm per coordinate.

This number reflects the sum of the StarScan measure errors and the errors inherent in the photographic material, and is dominated by the grain noise of this type of emulsion, consistent with previous investigations (Auer & van Altena 1978). However, these numbers do not directly translate into α, δ accuracies. In order to get highly accurate astrometric positions on the sky from these calibrated, measured x, y data the systematic errors introduced by the astrograph (optics, guiding, etc.) and the atmosphere need to be detected, quantified, and removed.

5.2. Long-Term Repeatability and Discussion

A fine-grain (Kodak Technical Pan emulsion) plate (No. 724) of a dense field (NGC 6791) obtained at the Lick 50-cm astrograph has been measured multiple times during the StarScan operations at relatively regular intervals to monitor its performance. In contrast to to the DCP, the location of the dots on this plate are not known a priori; however, they are fixed and StarScan should measure the same positions of these stellar images (within its errors) every time it has been measured. Thus, these data sets provide information about the long-term stability and repeatability of the StarScan measures and shed some light on the validity of using the x, y-table correction pattern as derived in the previous section.

Results are given in Table 2 for measures 1, 6, 9, and a (lines 27 to 30), which correspond to 2004 May, 2004 September, 2005 September, and 2006 April, respectively. For each data set, the plate was measured in direct (000) and reverse (180) orientation, and the eight-parameter model was used in a least-squares adjustment in the transformation between the orientations x, y data after applying the same 2-dim table corrections as presented above to all measures.

Figure 7 shows the residuals of such a transformation for the measure 6 (2004 September) of that Lick plate. As an example the x residuals are shown as a function of x, y, and magnitude. There is a magnitude equation of about 0.3 μm amplitude for x, while there is none for the y coordinate (not shown here). Residuals as a function of the coordinates still show systematic errors up to about 0.5 μm, even after applying the 2-dim x, y table corrections. The high-frequency wiggles are likely caused by the residual CCD camera mapping errors, while the low-frequency systematic errors are likely deviations of

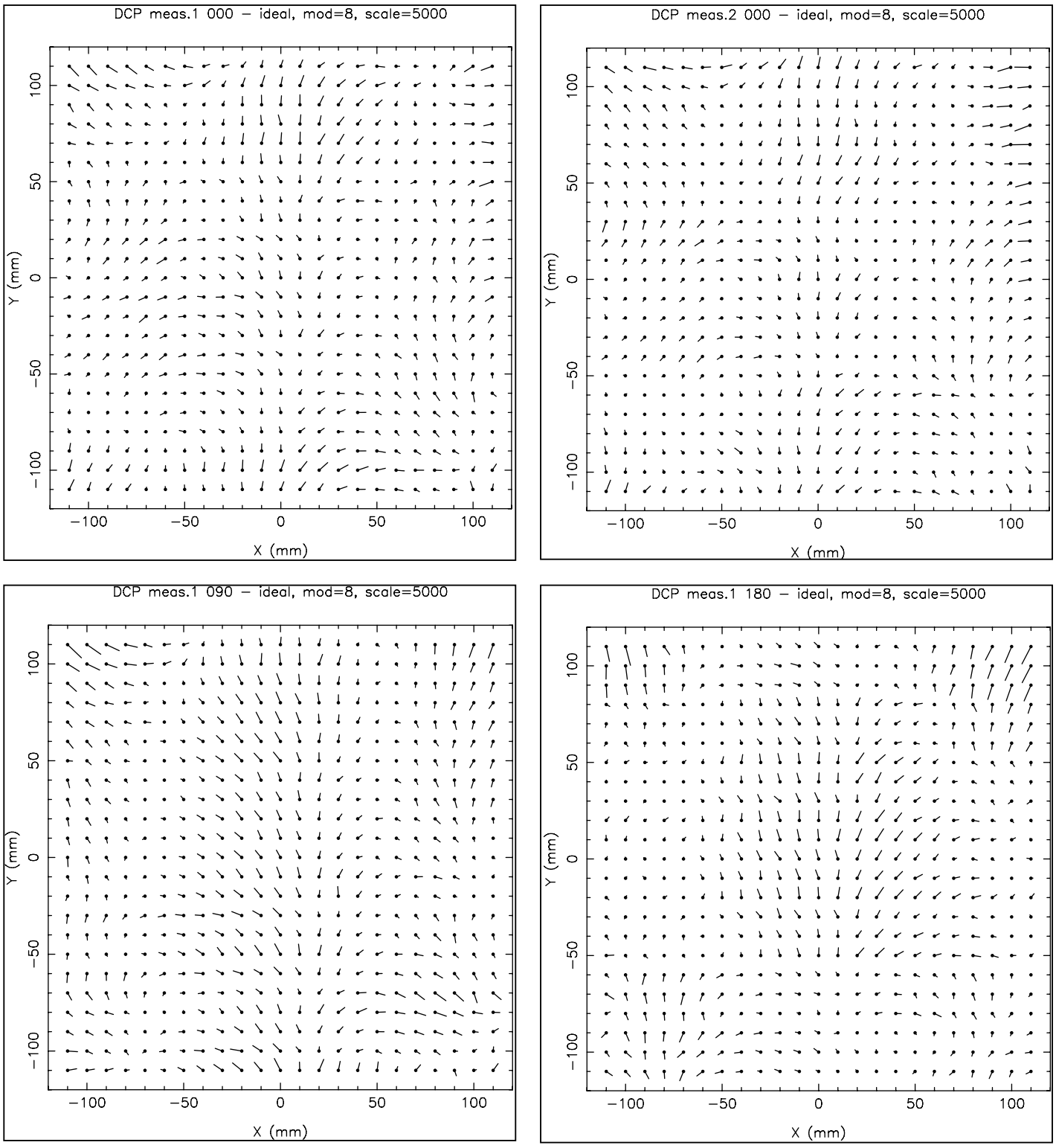

FIG. 5.—Differences between individual orientation measures of the DCP and the ideal grid coordinates after a least-squares fit with an eight-parameter transformation model. The scale is 5000; thus, the largest vectors are about 1.5 μm long. The top plots show results for the same orientation (0°) from the first and second set. The plots at the bottom show more results from the first set for the 90° and 180° orientation measures.

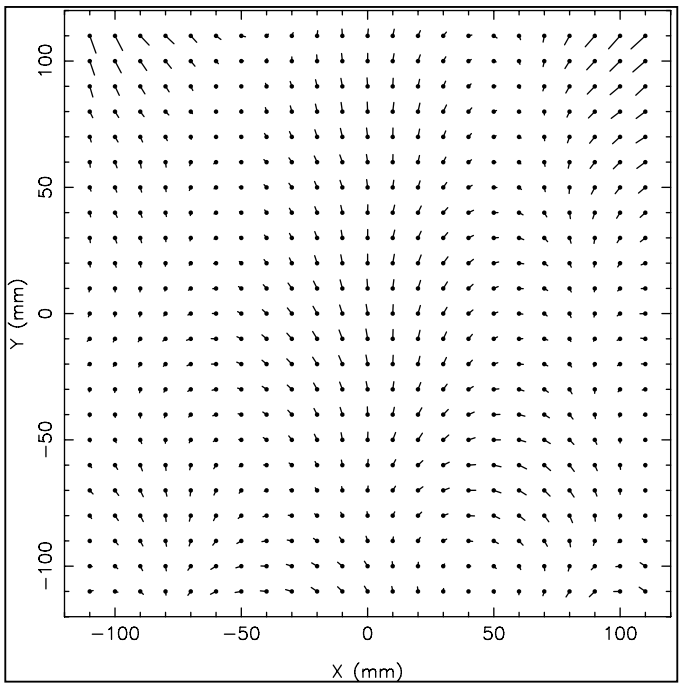

FIG. 6.—Mean StarScan x, y-table corrections. This pattern was derived by taking the smoothed average over all eight vector plots, of which some are shown in Fig. 4. The scale is 5000; thus, the largest vectors are about 1.0 μm long.

the x, y-table corrections as applied with respect to what actually is inherent in the data at the time of the measurement.

In order to better illustrate the long-term variability, Figure 8 shows only the x residual versus y plot but for three other measures of the same plate (2004 May, 2005 September, and 2006 April), which should be compared to the middle diagram of Figure 7. Clearly there are variations over time; however, the overall correction is good to about 0.4 μm per coordinate, with the rms error being much smaller.

Part of the remaining systematic pattern is clearly correlated with the location of stellar images on the CCD area. This is caused by an imperfect model in mapping from the CCD pixel coordinates to the x, y-table coordinate system. This is not surprising considering that the poorest image quality of the CCD area (their corner and border areas) are utilized to determine those mapping parameters, and an extrapolation to the entire CCD area has to be made. Measuring plates with significantly larger overlap between adjacent CCD images would help to lower those type of errors. However, as other error sources indicate, we have reached the overall StarScan accuracy limit and allowing a significantly larger overlap would have increased the project time significantly with little benefit. The HAM-I measuring machine (Zacharias et al. 1994) completely eliminated this problem by centering each star to be measured on the CCD image. However, that required an a priori measure list and a very long measure time, but an astrometric accuracy similar to that of StarScan was obtained.

It is not possible to correct the measures for the remaining systematic errors as a function of the coordinates based on findings like those shown in Figures 7 and 8 because the *differences* between the direct and reverse measure are seen here, while the combined, mean measured position of each star would be based on the *sum* of the measures. Comparisons like these for the residuals as a function of the coordinates serve as a check of the data and applied models and are indicative for such systematic errors staying constant, which allows us to group plate measures correctly in further reduction steps.

The situation is much different for the magnitude-dependent systematic errors. Assuming that the magnitude equation is constant for both orientation measures, it automatically drops out when combining the direct and reverse measures, while twice the deviation of a single measure with respect to the error-free data is seen in the residual plot as a function of magnitude. If only a single plate orientation were measured, this magnitude equation would need to be determined and corrected by some other means, which would be hard to do.

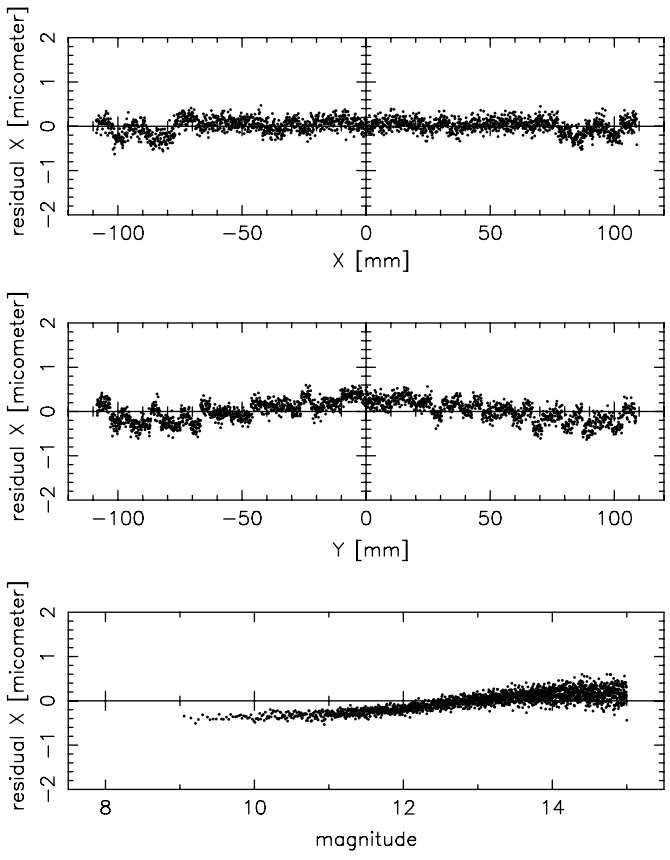

FIG. 7.—Data of Lick Astrograph plate 724 measured in two orientations in 2004 September (measure no. 6). The "direct" minus "reverse" residuals in x are shown as a function of x, y, and magnitude (top to bottom). Each dot is the average over 25 stars, thus highlighting the systematic errors.

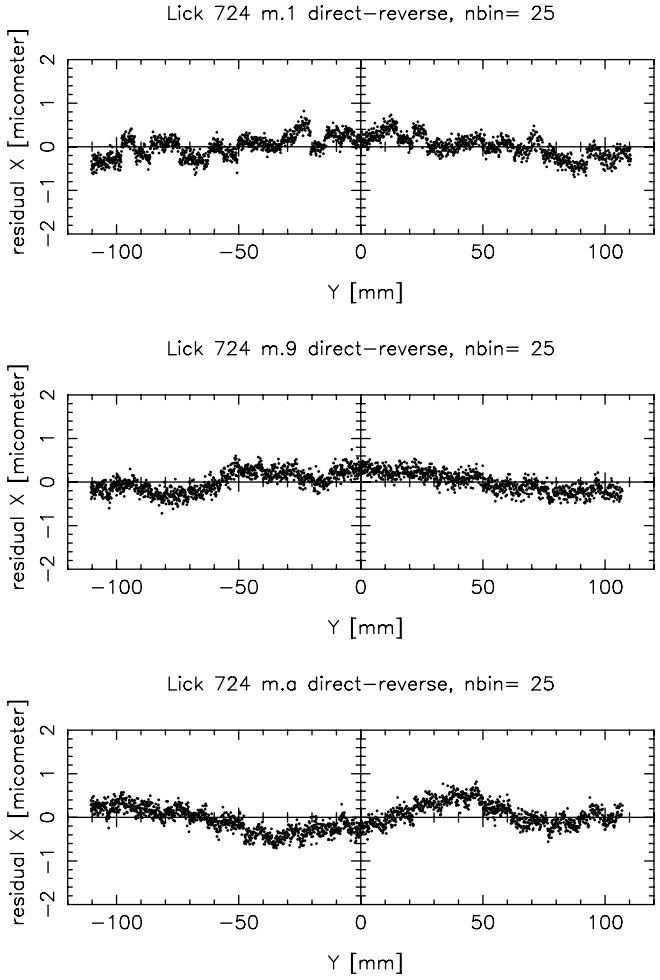

FIG. 8.—Data of Lick Astrograph plate 724 measured in two orientations. The direct minus reverse residuals in x are shown as a function of y for three different measure dates (from top to bottom): 2004 May (m.1), 2005 September (m.9), and 2006 April (m.a) Each dot is the average over 25 stars, thus highlighting the systematic errors.

6. SUMMARY AND CONCLUSIONS

For well-exposed stellar images, StarScan has a repeatability error of 0.2 μm per coordinate. Using overlapping areas in the digitization process, the mapping parameters of the CCD camera with respect to the x, y-table coordinate system are calibrated for each plate and orientation measure to the same precision. The overall accuracy of StarScan measures is limited by the systematic errors of the x, y-table and the stage motions. Using a dot calibration plate specifically manufactured for this purpose, two-dimensional correction data are obtained to calibrate the x, y-table coordinate system. The high precision of the StarScan measures allows one to see in this calibration pattern variations that depend at least on time, maybe on other parameters as well. The uncalibrated machine performs at an accuracy level of about 1 μm rms with a parabola-like distortion for the Δy as a function of y, with ± 1.5 μm amplitude being the largest error contribution. After applying the 2-dim calibration corrections StarScan performs at an accuracy level of 0.3 μm per coordinate.

By comparing different photographic plates of the same field, it has been demonstrated that astrometric useful information at an accuracy level of at least 0.65 μm can be extracted from the data of coarse-grain emulsions exposed at dedicated astrographs. Comparisons of direct and reverse measures of fine-grain emulsions show errors of 0.3 μm per single star image and measure. This is only an upper limit of the plate data quality, because of StarScan measuring machine errors close to the same level. A higher accuracy than StarScan currently can provide is recommended for fine-grain astrometric plates, and such a new machine was just delivered to the Royal Observatory Belgium (De Cuyper & Winter 2006).

It is recommended to measure the dot calibration plate often to verify and improve the 2-dim x, y-table corrections. Measuring a plate in two orientations, rotated by 180°, is mandatory, at least for StarScan and when aiming at high-accuracy metric results, in order to correct for the nonlinear magnitude equation from the measure process and to monitor quality by identifying occasional problems in the measure process.

The authors thank Sean Urban, who oversaw the operations in the past. Brian Mason and William Hartkopf are thanked for assisting in the daily measure effort. John Pohlman and Gary Wieder, former and current head of the USNO instrument shop, and all instrument shop personnel involved in the StarScan program are thanked for their effort in maintaining and upgrading the machine. Steven Gauss, former head of the Astrometry Department, is thanked for his support of StarScan, particularly in managing to keep the machine alive. Ralph Gaume, current head of the Astrometry Department, is thanked for his support, in particular for budgeting several contracts that allowed the maintenance and upgrade of StarScan. Hamburg Observatory (director Prof. Schmidt) is thanked for loaning the Zone Astrograph plates to USNO for digitization.

REFERENCES

Auer, L. H., & van Altena, W. 1978, AJ 83, 531
De Cuyper, J.-P., & Winter, L. 2006, in ASP Conference Series 351, Astronomical Data Analysis and Software System (ADASS) XV, ed. C. Gabriel, C. Arviset, D. Ponz, & E. Solano (San Francisco: ASP), 587
Douglass, G. G., & Harrington, R. S. 1990, AJ 100, 1712
ESA 1997, The Hipparcos Catalogue (ESA SP-1200; Garching: ESA)
Høg, E.et al. 2000, A&A, 355, L27
Schorr, R., & Kohlschütter, A. 1951, Zweiter Katalog der Astronomischen Gesellschaft, AGK2, Volume I (Hamburg: Bonn and Hamburg Observatories)
de Vegt, C. 1976, Mitt. Astron. Ges., 38, 181

———. 1978, in IAU Col. 48, Modern Astrometry, ed. F. V. Prochazka, & R. H. Tucker (New York: Springer), 527
Winter, L. 1999, Ph.D. thesis, University of Hamburg
Winter, L., & Holdenried, E. 2001, BAAS, 33, 1494
Zacharias, M. I., et al. 2000, AJ, 120, 2131
Zacharias, N., Urban, S. E., Zacharias, M. I., Wycoff, G. L., Hall, D. M., Monet, D. G., & Rafferty, T. J. 2004, AJ 127, 3043
Zacharias, N., de Vegt, C., Winter, L., & Weneit, W. 1994 in IAU Sympos. 161, Astronomy from Wide-Field Imaging, ed. H. T. MacGillivray, et al. (Dordrecht: Kluwer Acad. Publ.), 285
Zacharias, N., & Zacharias, M. I. 1999, AJ, 118, 2503